第 31卷 第 1期
2010年 1月
焊 接 学 报
TRANSACTIONS OF THE CHINA WELDING INSTITUTION
Vol 31 No. 1
January 2010

# 输气管线在役焊接管道内壁变形的数值模拟

陈玉华[1,2]， 王 勇[2]， 何建军[3]
(1. 南昌航空大学 航空制造工程学院，南昌 330063; 2. 中国石油大学 机电工程学院，山东 东营 257061;
3. 中国工程物理研究院，四川 绵阳 621907)

**摘 要**：采用焊接过程数值模拟软件 SYSWELD研究了输气管线在役焊接过程中管道内壁的变形，并和常规焊接进行了对比. 结果表明，对于在役焊接近缝区的一点，随着焊接热源的靠近，变形量逐渐增大，当焊接热源经过该点时变形量最大，在随后的冷却过程中，变形量减小. 在役焊接时焊接接头的变形与常规焊接有较大差异，在役焊接过程中接头的瞬态变形和残余变形均为外凸变形；而对于常规焊接，随着焊接冷却过程的进行，逐渐由外凸变形过渡为内凹变形，最终的残余变形为内凹变形. 随着焊接热输入的增大，在役焊接接头近缝区的瞬态变形和残余变形均增大，远离焊缝中心区域的瞬态变形和残余变形随着热输入的增加而减小.

**关键词**：在役焊接；气管线；变形；数值模拟
**中图分类号**：TG402 **文献标识码**：A **文章编号**：0253 - 360X(2010)01 - 0109 - 04

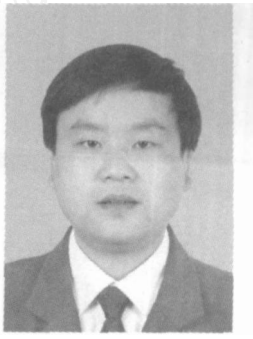

陈玉华

## 0 序 言

对需要修复的输气管线进行在役 (不停输、带压)焊接修复可保持管道运行的连续性、避免停输所造成的损失[1,2]. 然而，金属材料的强度随着温度的升高而急剧降低，例如，对普通碳钢材料，400 ℃时的屈服强度约为室温时的一半，而在 800 ℃时基本处于塑性状态，强度约为室温时的 4%～10%[3]. 输气管线在役焊接修复时，焊接区的管道从外表面到内表面沿壁厚方向一部分区域处于熔融状态、已完全丧失承载能力，一部分区域温度处于 400 ℃以上、强度下降，明显降低了管道的原有承载能力. 当焊接区剩余壁厚不足以承受介质压力及焊接应力的共同作用，就会发生烧穿 (管壁穿孔)，引起气体的泄漏，轻则导致在役焊接修复的失败，重则会引起爆炸[4,5]. 因此，防止烧穿是在役焊接修复考虑的首要问题，引起了各国从事在役焊接研究专家的重视，但大多以试验研究为主，并采用管道内壁峰值温度不超过 982 ℃作为避免烧穿的依据[6].

实际上，烧穿是由于管壁在管道内气体压力和焊接应力的共同作用下沿径向发生的外凸变形量超过一定限度而引起的. 因而，文章从气管线在役焊接过程中的变形来探讨烧穿问题，采用焊接过程数值模拟软件 SYSWELD计算在役焊接过程中的变形，和常规焊接 (即焊接时管道内无气体介质)进行对比，并探讨焊接热输入对在役焊接瞬态变形和残余变形的影响规律.

## 1 在役焊接数值模型的建立

### 1.1 几何模型

所有建模和计算均采用焊接过程数值模拟软件 SYSWELD进行. 采用图 1所示的套管修复工艺，其焊接接头横截面如图 2所示，由于烧穿一般发生在第一道焊缝，因此研究焊接接头第 1道焊 (即在管道外表面堆焊环焊缝)时管道内壁的径向变形. 由

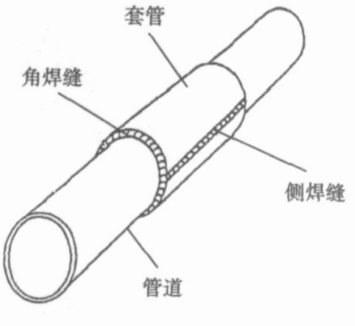


图 1 套管修复示意图

Fig. 1 Sketch map of sleeve repair

收稿日期：2008 - 09 - 12

于管道的轴对称性,可采用 1/2模型,二维截面网格模型如图 3所示,OA为管道内壁,BC为外表面,OB为焊接接头横截面的中心线. 管道长度取 200 mm,壁厚 8 mm,管道外径 508 mm.

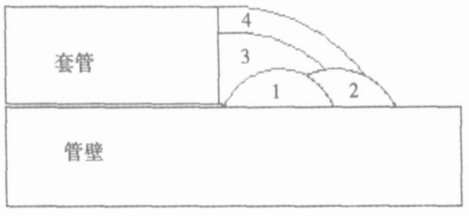


图2 焊接接头示意图

Fig. 2 Sketch map of welded joint

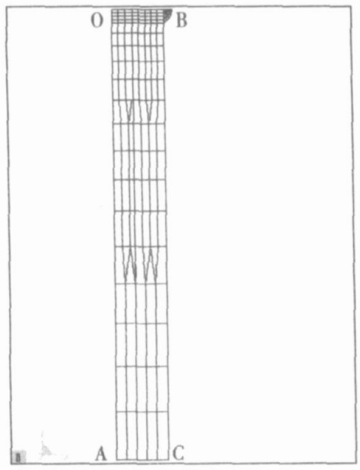


图3 二维横截面有限元网格模型

Fig. 3 Finite element model of 2D cross-section

### 1.2 焊接热源模型

由于双椭球模型更为准确[7],焊接热源采用双椭球模型. 采用焊条电弧焊方法,根据不同电流下焊接熔池的深度和宽度初步确定双椭球热源模型的各参数,然后采用 SYSWELD的热源拟合工具进行多次校核,直至模拟出的熔池形状和实际接头相符. 采用的四种热输入及相关工艺参数见表 1.

表 1 焊接工艺参数

Table 1 Welding parameters

| 工艺参数编号 | 焊接电流 $I$/A | 电弧电压 $U$/V | 焊接速度 $v$/(mm·s$^{-1}$) | 热输入 $E$/(kJ·cm$^{-1}$) |
|---|---|---|---|---|
| A | 85 | 28 | 4 | 6.0 |
| B | 110 | 28 | 3.3 | 9.3 |
| C | 130 | 29 | 3.4 | 11.1 |
| D | 150 | 30 | 3.4 | 13.2 |

### 1.3 换热边界条件及约束

管道外表面和空气的换热主要考虑辐射换热和空气的自然对流换热,总换热系数为

$$\alpha = 0.8 \times 5.67 \times 10^{-8}[(273.15+T_0)+(273.15+T)]\cdot[(273.15+T_0)^2+(273.15+T)^2]+25 \quad (1)$$

式中: $T_0$, $T_1$ 分别为环境温度 (25 ℃)和焊接接头与空气接触表面的温度 (℃).

在役焊接接头背面 (即管道内壁)和气体间的换热为管内强迫对流换热,其换热系数为

$$\alpha_1 = 0.027\frac{\lambda}{d}Re^{0.8}Pr^{1/3}\left(\frac{\mu}{\mu_w}\right)^{0.14} \quad (2)$$

式中:$\lambda$, $Re$, $Pr$, $\mu$ 分别为气体的导热系数、雷诺数、普朗特数、动力粘度; $d$为管道的内径; $\mu_w$ 为气体在壁温时的动力粘度.

$$\mu_w = \mu_0\left(\frac{273.15+T_1}{273.15}\right)^{0.76} \quad (3)$$

式中: $T_1$ 为管道内壁的温度 (℃); $\mu_0$ 为气体 0 ℃时的动力粘度. 管道内的气体介质为甲烷,其热物理性能参数参照文献[8]的数据确定.

### 1.4 X70管线钢的热物理性能及力学性能

X70管线钢的导热系数和比热采用文献[9]的公式计算得到,力学性能采用文献[10]提供的数据.

## 2 计算结果分析与讨论

考察图 3中所示管道内壁横截面 (OA方向)在焊接开始后 1 s(时刻 Ⅰ)、焊接热源经过该截面的时刻 (时刻 Ⅱ,即焊接开始后 120.9 s)、焊接刚刚结束的时刻 (时刻 Ⅲ,即焊接开始后 241.8 s)和 1 000 s (时刻 Ⅳ)四个时刻的变形,其中时刻 Ⅰ, Ⅱ, Ⅲ代表焊接过程中三个典型时刻的瞬态变形,时刻 Ⅳ的变形为焊后的残余变形.

### 2.1 在役焊接时管道内壁的变形过程

当气体流速为 15 m/s,压力为 6 MPa,采用表 1中 D组焊接工艺参数时,所考察的横截面的管道内壁在 Ⅰ, Ⅱ, Ⅲ, Ⅳ各时刻变形如图 4所示. 可以看出,时刻 Ⅰ,虽然焊接热源还未对所考察的横截面产生影响,但管道内部的压力已经引起了管道内壁约 0.2 mm的变形量. 时刻 Ⅱ,焊接热源作用于所考察的横截面,此时熔深最深,焊接温度场处于充分发展阶段,焊接区管壁的强度最低,因而引起的变形量最大,在焊缝中心正下方最大变形量达 0.52 mm,随着离焊缝中心距离的增加,变形量较小. 焊后冷却过程中,随管道内壁位置的不同变形量发生了较大的变化. 时刻 Ⅲ和时刻 Ⅳ,焊缝中心正下方的变形量不再是最大,而是最小,变形量几乎为零. 随着离焊缝中心距离的增加,变形量先增大并在 6 mm处达

最大值,然后减小至 30 mm处达最小值,随后再次增大.

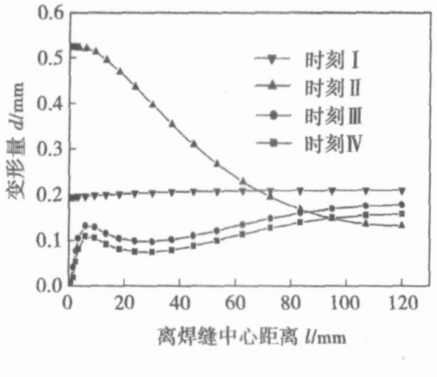


图 4　在役焊接时管道内壁各时刻的变形量

Fig. 4　Pipe inwall deformation of in-service welding at different times

对于近缝区一点,其变形过程为:随着焊接热源的靠近,变形量逐渐增大,当焊接热源经过该点所在的管道横截面时的变形量达到最大;在随后的冷却过程中,变形量不断减小. 总的看来,在该条件下,输气管线在役焊接管道内壁的瞬态变形和残余变形相对管道原始尺寸均为外凸变形.

### 2.2　在役焊接变形和常规焊接对比

对于常规焊接,在时刻 Ⅰ,由于焊接热源未开始作用,而且也无其它外界作用,其变形量为零. 时刻 Ⅱ,Ⅲ和 Ⅳ,在役焊接时管道内壁各点的变形与相同条件下(壁厚 8 mm,管道外径 508 mm,D组焊接工艺参数)常规焊接对比如图 5所示.

从图 5可以看出,时刻 Ⅱ,在役焊接变形量沿管道内壁各点分布曲线的形态和常规焊接类似,只是数值上要比常规焊接大 0.13～0.18 mm,而且距离焊缝中心越近其差值越大. 时刻 Ⅲ,在距离焊缝中心 70 mm以内的区域,常规焊接的变形量要大于在役焊接,而在 70 mm以外的地方,在役焊接的变形量要大于常规焊接. 其原因是在距离焊缝较近的区域焊接热作用以及随后的冷却过程造成的变形较强烈,在役焊接管内气体介质通过影响冷却过程而影响了其变形;在远离焊缝中心的区域,焊接热作用不明显,造成变形量差异的主要原因是在役焊接管内气体的压力. 时刻 Ⅳ,常规焊接管道内壁产生了较大的内凹变形,焊缝中心正下方的内凹变形量最大,达 0.43 mm. 随着离焊缝中心距离的增大,内凹变形量减小. 对于在役焊接,除了焊缝中心正下方微小区域内变形基本为零外,其余区域均为外凸变形,且变形量较小,最大值为 0.15 mm左右.

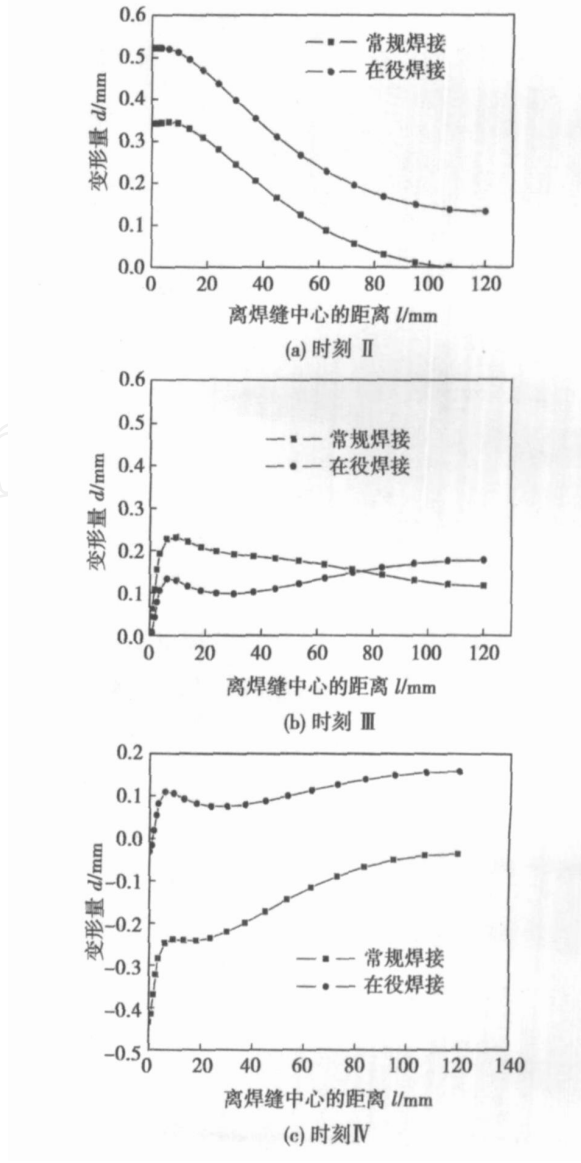


图 5　在役焊接和常规焊接变形量对比

Fig. 5　Comparison of deformation between in-service welding and routine welding

总之,在役焊接和常规焊接的瞬态变形和残余变形有较大差异. 在役焊接过程中的瞬态变形和残余变形均为外凸变形;而对于常规焊接,随着焊接冷却过程的进行,逐渐由外凸变形过渡为内凹变形,最终的残余变形为内凹变形.

### 2.3　热输入对在役焊接接头变形的影响

在相同的管道结构因素(壁厚 8 mm,管道外径 508 mm)、气体压力 6 MPa和气体流速 8 m/s时,分别按表 1中四组工艺计算管道径向变形沿管道内壁的分布,并进行比较,结果见图 6. 从图中可以看出,时刻 Ⅱ时,各种热输入下径向变形均为外凸变形,近缝区变形量随着热输入的增大而增大,远离焊缝中心区域的变形量不受热输入的影响. 时刻 Ⅲ和时刻 Ⅳ时,变形相对时刻 Ⅱ大大减小,近缝区的变形随着

焊接热输入的增加而增大;在离焊缝较远的区域(20 mm以外的区域),变化规律与之相反,变形随着热输入的增加而减小.

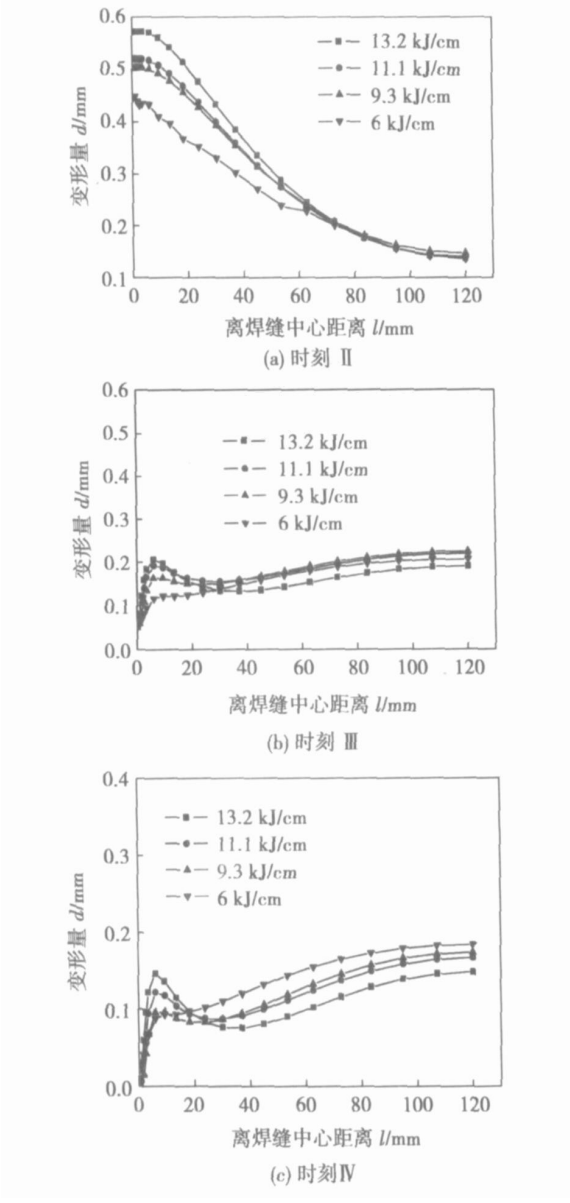


**图 6 焊接热输入对变形量的影响**

Fig. 6 Influence of heat input on deformation

## 3 结 论

(1) 在所选取的条件下,在役焊接近缝区一点的变形过程为:随着焊接热源的靠近,变形量逐渐增大,当焊接热源经过该点所在的管道横截面时的变形量达到最大,在随后的冷却过程中,变形量减小,最终的残余变形量小于初始时刻的变形量.

(2) 在役焊接时接头的瞬态变形、残余变形与常规焊接有较大差异. 在役焊接过程中接头的瞬态变形和残余变形均为外凸变形;而对于常规焊接,随着焊接冷却过程的进行,逐渐由外凸变形过渡为内凹变形,最终的残余变形为内凹变形.

(3) 随着焊接热输入的增大,在役焊接近缝区的瞬态变形和残余变形均增大,远离焊缝中心区域的瞬态变形和残余变形随着热输入的增加而减小.

## 参考文献:


[1] 陈玉华, 王 勇. 基于 SYSWELD的运行管道在役焊接热循环数值模拟 [J]. 焊接学报, 2007, 28(1): 85 - 88.
Chen Yuhua, Wang Yong. Numerical simulation of thermal cycle of In-service welding onto active pipeline based on SYSWELD [J]. Transaction of the China Welding Institution, 2007, 28(1): 85 - 88.

[2] 陈玉华, 王 勇, 韩 彬. X70管线钢在役焊接局部脆化区的组织及精细结构 [J]. 材料热处理学报, 2007, 28(1): 77 - 80.
Chen Yuhua, Wang Yong, Han Bin. Metallurgical microstructure and fine structure in local brittle zone of in-service welding of X70 pipeline steel[J]. Transaction of Materials and Heat Treament, 2007, 28(1): 77 - 80.

[3] Bout V S, Gretskii Y Y. 电弧焊在运行管道上的应用 [C] // 95 国际管道技术会议论文集. 北京: 1996: 398 - 404.

[4] 陈玉华, 王 勇, 董立先, 等. 高压油气管线在役焊接修复技术进展 [J]. 压力容器, 2005, 22(2): 36 - 40.
Chen Yuhua, Wang Yong, Dong Lixian, *et al*. Advance on repair of pressurized oil and gas pipelines by in-service welding technology[J]. Pressure Vessel technology, 2005, 22(2): 36 - 40.

[5] Otegui J L, Cisilino A, Rivas A, *et al*. Influence of multiple sleeve repairs on the structural integrity of gas pipelines[J]. International Journal of Pressure Vessels And Piping, 2002, 79(11): 759 - 765.

[6] William A Bruce. Repair of in-service pipelines by welding[J]. Pipes & Pipelines International, 2001, 46(9 - 10): 5 - 11.

[7] 莫春立, 钱百年, 国旭明, 等. 焊接热源计算模式的研究进展 [J]. 焊接学报, 2001, 22(3): 93 - 96.
Mo Chunli, Qian Binian, Guo Xuming, *et al*. Research status of welding resource computer method[J]. Transaction of the China Welding Institution, 2001, 22(3): 93 - 96.

[8] 任 瑛, 张 弘. 传热学 [M]. 东营: 石油大学出版社, 1988.

[9] 余大涛. 高性能管线钢受焊区的脆化规律与组织、性能的理论模拟和预测 [D]. 西安: 西安石油学院, 2002.

[10] Bang I W, Son Y P, Oh K H, *et al*. Numerical simulation of sleeve repair welding of in-service gas pipelines [J]. Welding Journal, 2002, 81(12): 273 - 282.


**作者简介**: 陈玉华,男,1979年出生,工学博士,副教授. 主要从事材料焊接性、特种焊接技术和金属表面工程方面的科研和教学工作. 发表论文 40余篇.

Email: ch_yu_hu@163.com

wavelet basic waves are used to analyze the $CO_2$ arc voltage signal in Matlab, finally the db2 basic wave is selected and used in this algorithm in which the filter is stationary and the sampling signal is processed one by one by three-decomposition. To meet real-time requirements, the main program is developed in C++ and the assembly subroutine of wavelet detection is developed by the multiplier of DSP and the RPT instruction. As a result, it has a fast operation speed and improves the real time capability of detection. The calculation results of C++ program show the accuracy and the feasibility of this algorithm. Experiment results show that false short-circuit signal can be removed by the db2 basic wave and the short-circuit moment can be decteted in real time by this algorithm.

**Key words:** wavelet transform; detection of short-circuit signal; algorithm; real-time

**Liquid crystal display system for spot welding current waveform and its amplitude-frequency diagram** ZHANG Yong, MA Tiejun, JIA Jingbo, YANG Siqian, XIE Hongxia (Shaanxi Key Laboratory of Friction Welding Technologies, Northwestern Polytechnical University, Xi'an 710072, China). p 97 - 100

**Abstract:** In order to on-line detect the diameter of the spot-welded nugget through the spectrum of the welding current, a liquid crystal displayer (LCD) system was developed to screen the welding current and its spectrum after fast fourier transformation (FFT). The digital signal processor (DSP) TMS320LF2407A and LCD TFTs6448b are indirectly interfaced to realize the data exchange with the same baud rate. Assembly language based program was embedded inside the C program to guarantee the real-time implementation of FFT. Experiments on spot weld of the mild steel with AC welding machine are pursued for the on-line status detection. The feasibility of the above displaying system in sample current collection, carrying out FFT, and displaying the waveform and its spectrum are validated.

**Key words:** spot welding; digital signal processor; fast fourier transformation algorithm; LCD display

**Analysis on welding stability of aluminum alloy pulse MIG welding based on approximate entropy** HUANG Jiankang[1], SHI Yu[2], NIE Jing[1], FAN Ding[2] (1. State Key Laboratory of Gansu Advanced Non-ferrous Metal Materials, Lanzhou University of Technology, Lanzhou 730050, China; 2. Key Laboratory of Non-ferrous Metal Alloys and Processing, The ministry of Education, Lanzhou University of Technology, Lanzhou 730050, China). p 101 - 104

**Abstract:** In order to evaluate the stability of aluminum alloy pulsed MIG welding, an approximate analysis has been done on voltage signal in the process of aluminum alloy pulsed MIG welding. The calculation and comparison of the approximate entropy on voltage signal under different welding procedures such as welding speeds, wire feed rate, duty cycle and so on, show that, the approximate entropy of voltage can reflect the stability of the process of aluminum alloy pulsed MIG welding. The results show that, the smaller the average value of approximate entropy and standard deviation is, the more stable the welding process will be. On the contrary, the welding process is unstable while the average value is high.

**Key words:** pulse MIG; approximate entropy; parameters; stability

**Seawater corrosion-resistant welding procedure of $00Cr_{18}Ni_{14}Mo_2Cu_2$ stainless steel** CHE Juntie[1], JI Zhongli[1], ZHANG Bing[1], HUANG Junhua[1] (1. China University of Petroleum, Beijing 102249, China; 2. Beijng Institute of Petro-chemical Technology, Beijing 102617, China). p 105 - 108

**Abstract:** In this paper, seawater corrosion-resistant welding procedure of $00Cr_{18}Ni_{14}Mo_2Cu_2$ austenitic stainless steel was studied. With the improvement of welding procedure, width of heat-affected zone (HAZ) was reduced, difference of chemical constitution between HAZ and fusion zone (FZ) was minished, metallurgical structure of HAZ was refined, precipitate of Fe-Cr phase ($\sigma$ phase) was controlled. The corrosion rate of HAZ was decreased and corrosion rate of weld joint (FZ, HAZ and base metal was emerged in corrosion liquor at the same time) was greatly decreased.

**Key words:** seawater corrosion, welding procedure, HAZ, corrosion rate

**Numerical simulation on deformation in inner pipe wall of in-service welding onto gas pipeline** CHEN Yuhua[1,2], WANG Yong[2], HE Jianjun[3] (1. School of Aeronautical Manufacturing Engineering, Nanchang Hangkong University, Nanchang 330063, China; 2. College of Mechanical and Electronic Engineering, China University of Petroleum, Dongying 257061, Shandong, China; 3. China Academy of Engineering Physics, Mianyang 621907, Sichuan, China). p 109 - 112

**Abstract:** The software of SYSWELD was used to simulate the welding deformation in inner pipe wall when in-service welding onto active gas pipeline and the deference of welding deformation between in-service welding and routine welding was compared. The results show that, for a point in the region near the in-service welded seam, its deformation increases when the welding heat source closes up, and achieves maximum when the welding heat source passes through this point. The deformation decreases during the cooling process. The deformation of in-service welded joint has much difference with routine welded joint. The transient deformation and residual deformation of in-service welded joint are all convex deformation, but the transient deformation of routine welded joint changes from convex deformation to concave deformation during the cooling process and the residual deformation is concave deformation. When heat input is increased, the transient deformation and residual deformation in the region near the in-service welded seam are also increasing, but the transient deformation and residual deformation in the region far from the in-service welded seam are decreasing.

**Key words:** in-service welding; gas pipeline; deformation; numerical simulation